Copper(II) bis(hexafluoroacetylacetonate) complexes with 2-(2-methyltetrazolyl)-4,4,5,5-tetramethyl-4,5-dihydro-1*H*-imidazole 1-oxides

E. V. Tretyakov,[a] S. V. Fokin,[a,b] G. V. Romanenko,[a] V. N. Ikorskii,[a,b] A. V. Podoplelov,[a] and V. I. Ovcharenko[a,b]★

[a] *International Tomography Center, Siberian Branch of the Russian Academy of Sciences, 3a ul. Institutskaya, 630090 Novosibirsk, Russian Federation. Fax: +7 (383) 333 1399. E-mail: Victor.Ovcharenko@tomo.nsc.ru*
[b] *Novosibirsk State University, 2 ul. Pirogova, 630090 Novosibirsk, Russian Federation*

An efficient procedure was developed for the synthesis of alkyltetrazolyl-substituted nitronyl nitroxides ($\mathbf{L^1}$ and $\mathbf{L^2}$). These compounds were used to prepare the first alkyltetrazolyl-substituted imino nitroxides ($\mathbf{L^3}$ and $\mathbf{L^4}$). The molecular structures of $\mathbf{L^3}$ and $\mathbf{L^4}$ were confirmed by X-ray diffraction. Investigation of the products prepared by the reaction of copper(II) bis(hexafluoroacetylacetonate), $Cu(hfac)_2$, with nitroxides made it possible to divide ligands $\mathbf{L^1}$—$\mathbf{L^4}$ into two groups. The reactions of spin-labeled tetrazoles $\mathbf{L^1}$—$\mathbf{L^3}$ with $Cu(hfac)_2$ afford the heterospin complexes $Cu(hfac)_2L_2$, whereas $\mathbf{L^4}$ serves as a bidentate ligand in the $Cu(hfac)_2\mathbf{L^4}$ complex. In the solid $Cu(hfac)_2L_2$ complexes, antiferromagnetic exchange interactions between the unpaired electrons of the nitroxide fragments of the adjacent molecules prevail, due to which μ_{eff} decreases with decreasing temperature, and the spins of nitroxides are completely compensated at 5—10 K. The $Cu(hfac)_2\mathbf{L^4}$ complex displays strong intramolecular ferromagnetic coupling, due to which μ_{eff} at room temperature is close to 2.9 μ_B.

Key words: nitroxide radicals, tetrazole, X-ray diffraction study, copper(II), heterospin complexes, magnetic susceptibility.

Progress in synthetic chemistry of nitroxides made it possible to perform the targeted design of molecular magnets.[1] For example, the efficient procedure, which has been developed for the synthesis of spin-labeled nitroxide, *viz.*, 2-cyano-4,4,5,5-tetramethyl-2-imidazoline-1-oxyl 3-oxide (**A**),[2] was successfully used for the preparation of the sodium salt of 4,4,5,5-tetramethyl-2-(1*H*-tetrazol-5-yl)-4,5-dihydro-1*H*-imidazole-1-oxyl 3-oxide and a related series of high-dimensional heterospin complexes.[3] Two isomeric nitroxides, *viz.*, 2-(1-methyl-1*H*-tetrazol-5-yl)- ($\mathbf{L^1}$) and 2-(2-methyl-2*H*-tetrazol-5-yl)-4,4,5,5-tetramethyl-4,5-dihydro-1*H*-imidazole-1-oxyl 3-oxides ($\mathbf{L^2}$), were prepared as a mixture of two isomers ($\mathbf{L^1}$ and $\mathbf{L^2}$) by methylation of the sodium salt of tetrazolyl-substituted nitronyl nitroxide, and their structures were determined. After recrystallization, these isomers can be separated only manually.[3] In the present study, we developed an efficient procedure for the preparation of isomers $\mathbf{L^1}$ and $\mathbf{L^2}$ in individual form. Then, we synthesized the corresponding imino nitroxides $\mathbf{L^3}$ and $\mathbf{L^4}$ from nitroxides $\mathbf{L^1}$ and $\mathbf{L^2}$ and studied their structures. Since the total series of spin-labeled 1- and 2-methyltetrazoles $\mathbf{L^1}$—$\mathbf{L^4}$ became accessible, we compared their behavior as ligands in reactions with copper(II) hexafluoroacetylacetonate, $Cu(hfac)_2$, and found that only one of these compounds ($\mathbf{L^4}$) has tendency to be coordinated in a bidentate fashion, whereas nitroxides $\mathbf{L^1}$—$\mathbf{L^3}$ form structurally similar heterospin complexes $Cu(hfac)_2L_2$ (**1—3**) with monodentate *trans*-coordinated nitroxides, which are bound through the donor N atoms of the tetrazole ring.

Results and Discussion

The lack of preparative procedures for the synthesis of individual nitroxides $\mathbf{L^1}$ and $\mathbf{L^2}$ did not allow researchers to study spin-labeled tetrazoles. Our experiments demonstrated that this problem can be most efficiently solved by excluding the previously used intermediate step of isolation of tetrazolide. The main steps, which enable one to prepare nitroxides $\mathbf{L^1}$—$\mathbf{L^4}$ in individual form, are presented in Scheme 1. Stirring of a solution of compound **A** in DMF containing a small excess of NaN_3 at 60—65 °C was accompanied by a gradual change in the color of the solution from blue-green to dark-blue. Within 3 h after complete consumption of the starting compound **A** (TLC control), an equivalent amount of Me_2SO_4 was added to

Published in Russian in *Izvestiya Akademii Nauk. Seriya Khimicheskaya,* No. 1, pp. 64—70, January, 2006.
1066-5285/06/5501-0066

the reaction mixture. Methylation occurs rapidly to form a mixture of isomers $\mathbf{L^1}$ and $\mathbf{L^2}$, which can easily be separated into individual components. Reduction of nitronyl nitroxides $\mathbf{L^1}$ and $\mathbf{L^2}$ with $NaNO_2$ affords methyltetrazole-substituted imino nitroxides $\mathbf{L^3}$ and $\mathbf{L^4}$, respectively. Single crystals of $\mathbf{L^1}$—$\mathbf{L^4}$ can be grown by slow evaporation of their solutions in a CH_2Cl_2—heptane mixture. Black rhombic platelet crystals of $\mathbf{L^1}$ gradually decompose even when stored in the dark at ~0 °C. Decomposition of small crystals occurs more rapidly and, after several months, these crystals are transformed into a yellow-brown amorphous substance. Under analogous conditions, larger crystals (1—4 mm) retain the shape, but their surface becomes covered with decomposition products. Dark-blue needle-like crystals of $\mathbf{L^2}$ and red-orange platelet crystals of $\mathbf{L^3}$ and $\mathbf{L^4}$ remain unchanged when stored in a refrigerator for one year.

Scheme 1

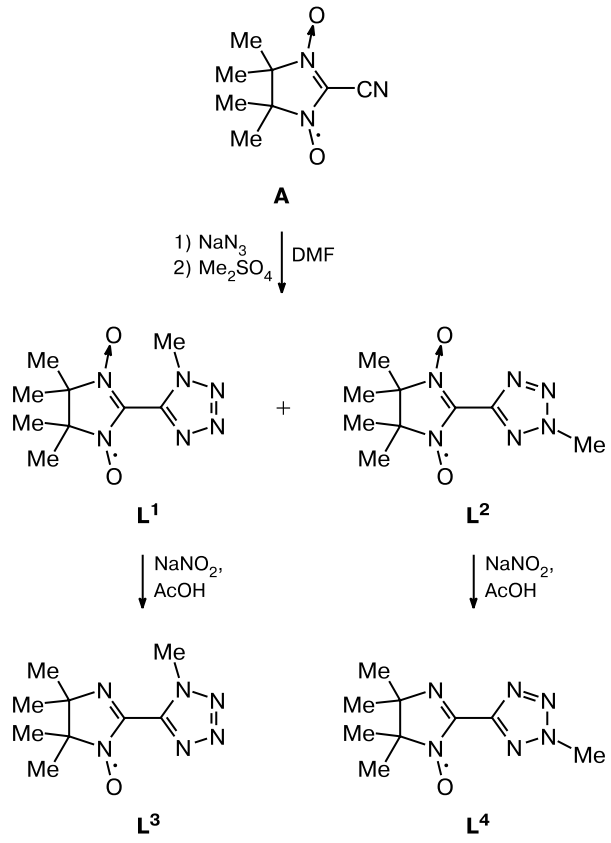

X-ray diffraction study of $\mathbf{L^3}$ and $\mathbf{L^4}$ demonstrated that, in spite of the difference in the position of the Me group in the tetrazole ring, the molecular packings in the crystals of these compounds differ only slightly (Fig. 1). The largest difference (Table 1) is observed for the angle between the planes of the tetrazole ring and the CN_2 fragment of the imidazoline ring ($\angle CN_2$—Tz). Due to the large value of this angle, the molecular shape can be described as a propeller, so that the molecular packing is characterized by a wave motif.

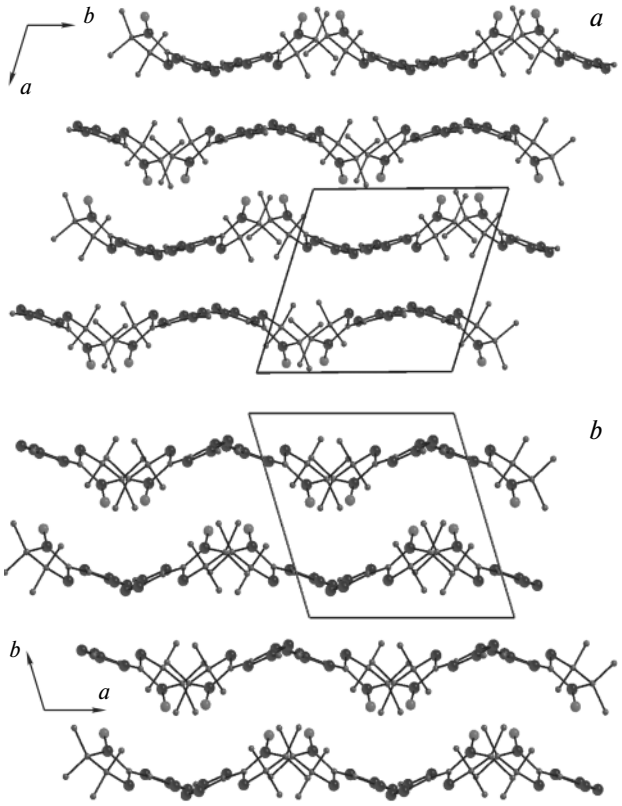

Fig. 1. Fragments of the crystal structures of $\mathbf{L^3}$ (*a*) and $\mathbf{L^4}$ (*b*).

Table 1. Selected bond lengths (*d*) and bond angles (ω) in molecules $\mathbf{L^3}$ and $\mathbf{L^4}$

L	*d*/Å				Angle CN_2—Tz /deg
	O—N	C—NO$^{\bullet}$	N—C	C_{Im}—C_{Tz}*	
$\mathbf{L^3}$	1.258(3)	1.379(4)	1.270(3)	1.456(4)	36.3(2)
	1.268(3)	1.388(3)	1.273(3)	1.451(4)	37.3(2)
$\mathbf{L^4}$	1.273(5)	1.403(6)	1.286(6)	1.452(7)	30.0(4)
	1.275(5)	1.379(6)	1.282(6)	1.454(7)	20.8(5)

* The atoms of the imidazoline (Im) and tetrazole (Tz) rings.

The reactions of $Cu(hfac)_2$ with nitroxides $\mathbf{L^1}$—$\mathbf{L^4}$ afford complexes, which rapidly decompose in solution to form a brown film on the walls of a reaction vessel. Nevertheless, we succeeded in finding conditions, in which the complexes can be crystallized, by varying the solvent ratio, the rates at which the solvents are removed, and the reaction temperature. Crystals of the $Cu(hfac)_2L_2$ complexes (L = $\mathbf{L^1}$ (**1**) or $\mathbf{L^2}$ (**2**)) were grown from a mixture of CH_2Cl_2 with hexane. Due to higher stability of complex **1**, good-quality crystals of this complex were grown.

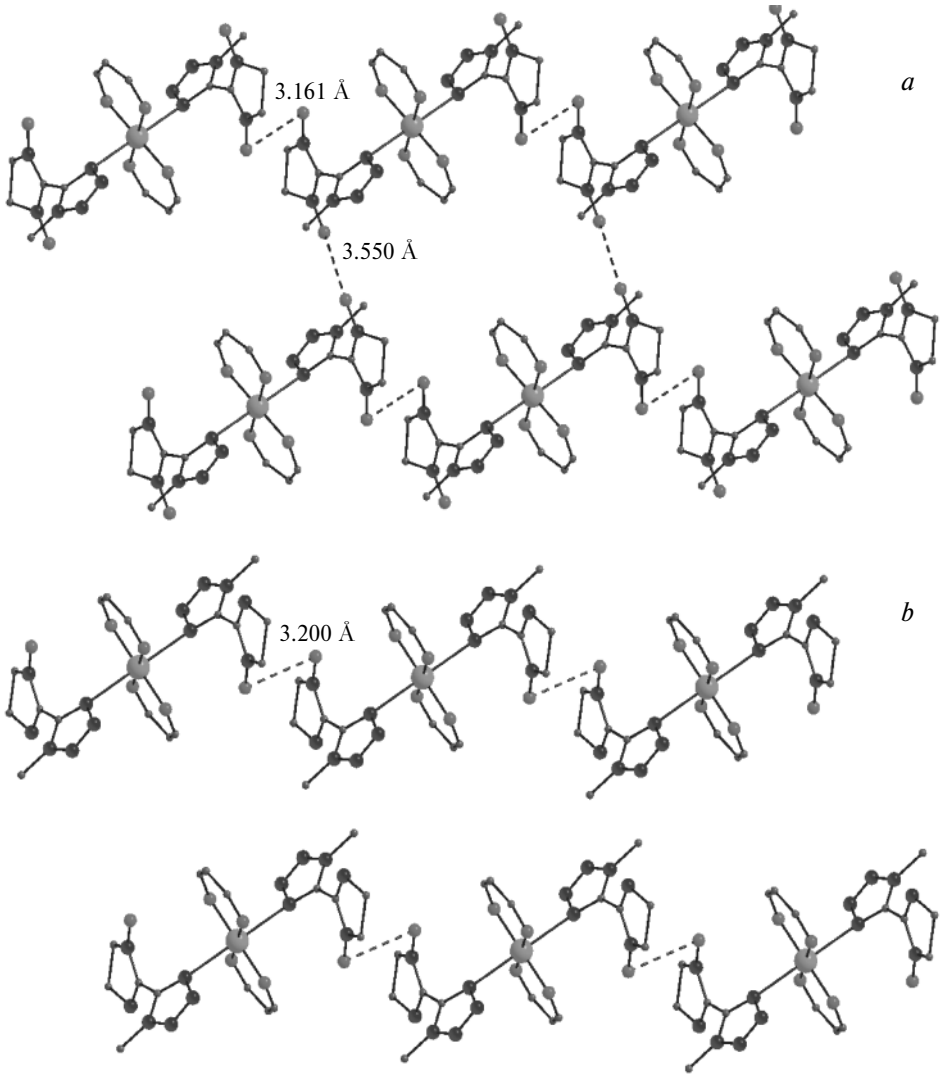

Fig. 2. Molecular packings in the crystal structures of **1** (*a*) and **3** (*b*). Intermolecular distances between the O atoms of the NO groups are indicated by dashed lines.

X-ray diffraction study demonstrated that complex **1** has a molecular structure (Fig. 2, *a*). The coordination environment of the central atom is a centrosymmetric axially elongated octahedron (Table 2), whose equatorial plane is formed by the O atoms of two hfac anions (*d*(Cu—O), 1.939—1.944 Å), and the axial positions are occupied by the N atoms of the tetrazole ring at distances of 2.477(3) Å. Since ligands $\mathbf{L^1}$ in complex **1** are optical isomers, the copper atom lies on an inversion center. The distances in the NO groups in molecules $\mathbf{L^1}$ are equal (see Table 2) and are typical of nitronyl nitroxides. The shortest intermolecular distances between the O atoms of the NO groups (see Fig. 2) are 3.161 and 3.550 Å.

The reaction of $Cu(hfac)_2$ with imino nitroxide $\mathbf{L^3}$ in a mixture of diethyl ether with hexane afforded the $Cu(hfac)_2\mathbf{L^3}_2$ complex (**3**). The molecular structure, molecular packing, and stereochemical characteristics of complex **3** are similar to those of complex **1** (see Table 2). The only difference is that the number of the shortest intermolecular contacts between the O atoms of the NO groups in complex **3** is half as large as that in complex **1** due to the absence of the N-oxide oxygen atom in molecule $\mathbf{L^3}$. It should also be noted that the twist angle of the heterocycles in complex **3** is substantially larger than that in free nitroxide $\mathbf{L^3}$ (*cf.* data from Tables 1 and 2).

The crystalline product, which was prepared by the reaction of $Cu(hfac)_2$ with $\mathbf{L^4}$ in hexane, contains two types of crystals, *viz.*, green elongated prisms (**4a**) and dichroic (green and brown faces in reflected light) prisms (**4b**) (see Table 2). The structure of complex **4a** consists of two crystallographically independent pairs of optical antipodes (Fig. 3).

To determine the conformation of coordinated molecule $\mathbf{L^4}$, it is convenient to consider both complexes

Table 2. Selected bond lengths (d) and bond angles (ω) in complexes **1—4**

Parameter	**1**	**3**	**4a**		**4b**	**4c**
Bond			d/Å			
$Cu—N_L$	—	—	2.037(4)	2.021(4)	2.050(2)	2.047(3)
$Cu—N_{Tz}$	2.477(3)	2.546(3)	2.562(4)	2.582(4)	2.536(2)	2.476(4)
$Cu—O_{hfac}$	1.939(2)	1.935(2)	1.946(3)	1.933(4)	1.931(2)	1.930(3)
	1.944(2)	1.941(2)	1.951(3)	1.936(4)	1.941(2)	1.950(3)
		1.987(3)	1.985(4)	2.002(2)	1.991(3)	
		2.235(3)	2.229(4)	2.207(2)	2.209(4)	
N—O	1.264(3)	1.267(3)	1.268(5)	1.266(5)	1.264(3)	1.258(4)
	1.261(3)					
—O˙...˙O—	3.161	3.200	—	—	—	—
	3.550					
Angle			ω/deg			
$CN_2—Tz$	55.4(2)	50.1(2)	6.6(5)	8.6(7)	5.9(2)	0.8(3)

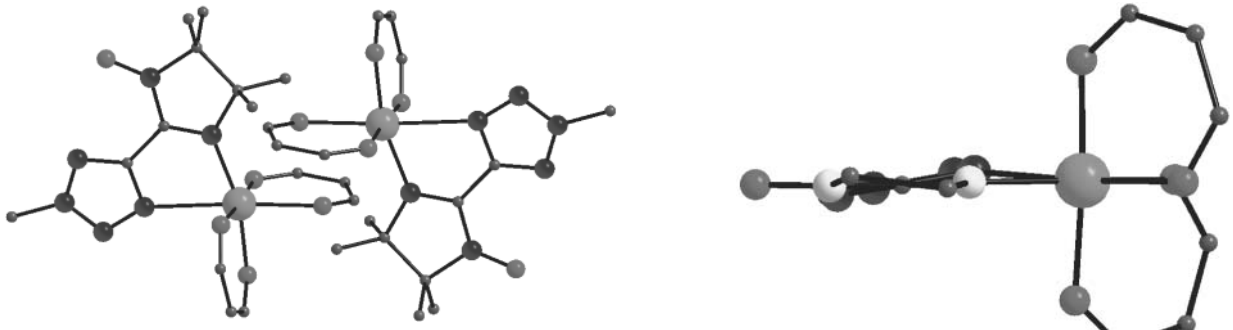

Fig. 3. Pair of optical isomers in the structure of **4a**.

along the line coinciding with the C—C bond, which links two heterocycles in ligand $\mathbf{L^4}$, as viewed from the imidazoline ring (Fig. 4). In coordinated molecule $\mathbf{L^4}$, the imidazoline fragment is twisted clockwise relative to the plane of the tetrazole ring. In addition, the carbon atom at position 5 of the imidazoline ring is located above the plane of the imino nitroxide fragment (N=C—N—O), whereas the carbon atom at position 4 is below this plane. Taking into account the stereochemical features of the molecular packing, the pairs of the $Cu(hfac)_2\mathbf{L^4}$ molecules (**4**) can exist as four combinations of optical antipodes, which differ in the configuration of the central metal ion (Λ or Δ), the sign of the twist angle of the heterocycles, which determines the configuration of the chiral center (*R* or *S*), and the half-chair conformation of the five-membered ring ((+)-synclinal or (−)-synclinal conformation as viewed along the bond between the carbon atoms at positions 4 and 5 of the imidazoline ring): 1) Δ*R*+sc—Λ*S*−sc; 2) Δ*R*−sc—Λ*S*+sc; 3) Δ*S*+sc—Λ*R*−sc; and 4) Δ*S*−sc—Λ*R*+sc. In the structure under consideration, one of such pairs is observed (see Fig. 4).

An analogous consideration of the second pair of optical isomers, which is also present in the structure of **4a**, shows that the imidazoline ring is planar, *i.e.*, the

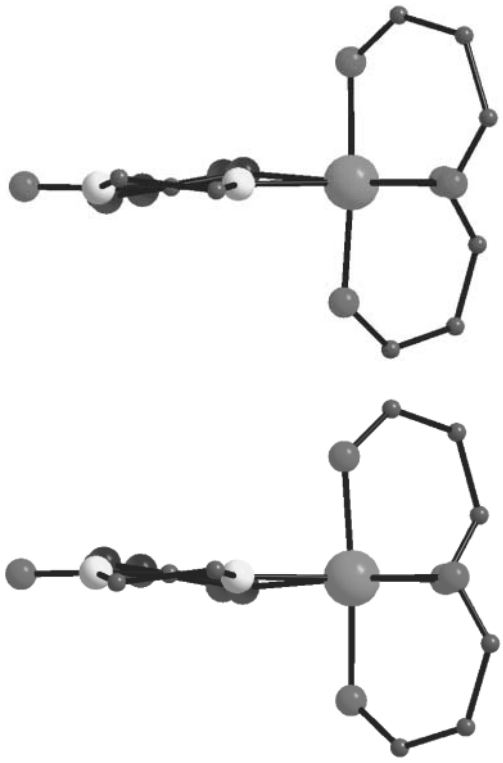

Fig. 4. Different conformations of molecules $\mathbf{L^4}$ in the pair of optical isomers of complex **4a** presented in Fig. 3.

Me groups at positions 4 and 5 of the imidazoline ring are in a synperiplanar conformation (Fig. 5).

X-ray diffraction study of crystals of **4b** showed that they contain a pair of optical antipodes stereoisomeric to the pair shown in Fig. 4.

Prolonged storage of crystals of **4a** and **4b** under the mother liquor afforded pale-brown platelet crystals of **4c**. Analogous crystals were obtained when a solution of $Cu(hfac)_2$ and $\mathbf{L^4}$ in hexane was warmed at 50—60 °C for

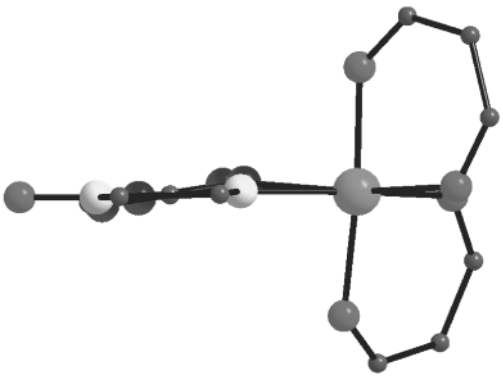

Fig. 5. Conformation of L^4 in the second crystallographically independent molecule of the complex in the structure of **4a**.

30—40 min followed by storage at room temperature for ≥3 h.

X-ray diffraction study of modification **4c** showed that its crystal structure also contains optical antipodes of the complex. In coordinated molecule L^4, the heterocycles lie in a single plane. In two molecules of the complex related by an inversion center, these pairs of ligands L^4 contain the imidazoline ring in different conformations (Fig. 6).

Therefore, high conformational flexibility of molecules L^4 is responsible for the formation of different modifications of complex **4**, some of which were isolated in the crystalline state.

The dependences $\mu_{eff}(T)$ for complexes **1**, **2**, and **3** are similar in character. Therefore, only the plots $\mu_{eff}(T)$ for complexes **1** and **4** are presented in Fig. 7. The effective magnetic moment of complex **1** at 300 K (2.97 μ_B) is equal to the spin-only value for three weakly coupled paramagnetic centers with the spins S = 1/2. The curve $\mu_{eff}(T)$ tends to the limit (~1.8 μ_B) with decreasing temperature, and then it again decreases at helium temperatures. This behavior is indicative of predominantly antiferromagnetic exchange interactions between the unpaired electrons of the paramagnetic centers in complex **1**, due to which the spins in two of three paramagnetic centers

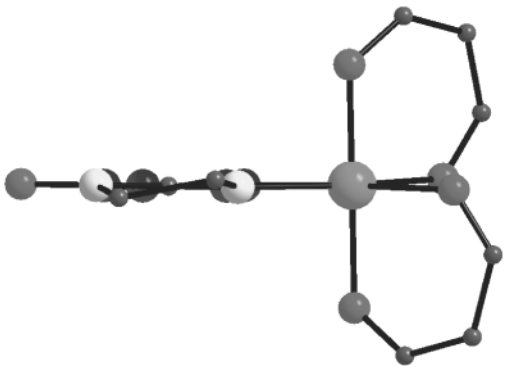

Fig. 6. Conformation of L^4 in complex **4c**.

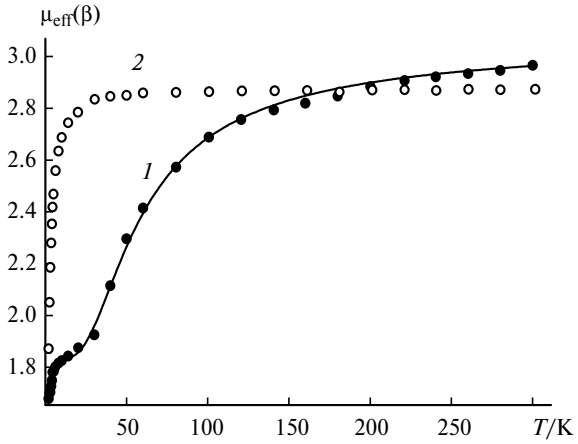

Fig. 7. Temperature dependences of the effective magnetic moments for complexes **1** (*1*) and **4** (*2*).

become paired upon cooling. A further decrease in μ_{eff} at helium temperatures is due to a weak intercluster exchange interaction.

Two alternative models can be considered for a theoretical description of the above dependences. According to one of these models, antiferromagnetic exchange interactions within the molecule occur through a long chain of atoms of the heterocycles. However, these exchange interactions are, as a rule, antiferromagnetic and have an energy of at most 1—3 cm^{-1}. Consequently, the observed character of the temperature dependence cannot be accounted for by these interactions. Another model is more reasonable and is consistent with the structural data (see Fig. 2). It assumes the presence of pair exchange interactions between the unpaired electrons of the adjacent rather closely spaced nitroxide groups. An analogous type of interactions with the energy of ≥50 cm^{-1} has been observed earlier.[4] We simulated the experimental temperature dependences with the use of Cu...[R—R] as the unit exchange cluster. The intercluster exchange interactions zJ' were taken into account by the molecular field method. The general principles of calculations of the magnetic properties of heterospin clusters with the use of the isotropic Hamiltonian were described in the study.[5] The theoretical dependence $\mu_{eff}(T)$ obtained by optimization is represented by a solid line in Fig. 7. Table 3 gives the optimal parameters of the model for complexes **1—3**.

Table 3. Optimal parameters of exchange interactions

Complex	g_{Cu}	$-J$	$-zJ'$
		cm^{-1}	
1	2.13	32.0	0.19
2	2.15	41.4	0.70
3	2.12	60.0	0.65

The effective magnetic moment of complex **4** (see Fig. 7, curve *2*), unlike μ_{eff} for complexes **1—3**, remains virtually unchanged (2.87 μ_B) as the temperature decreases from 300 to 50 K. Further cooling leads to a decrease in μ_{eff} to 1.87 μ_B. The value of the magnetic moment (μ_{eff} = 2.87 μ_B) and the fact that it remains constant down to low temperatures are indicative of strong intramolecular ferromagnetic exchange interactions (>300 cm^{-1}), with the result that complex **4** exists predominantly in the state with S = 1. A decrease in μ_{eff} at temperatures lower than 50 K occurs due to much weaker intermolecular antiferromagnetic exchange interactions.

Therefore, we developed an efficient procedure for the preparation of alkyltetrazolyl-substituted nitronyl nitroxides and synthesized the related imino nitroxides. Investigation of the products prepared by the reaction of $Cu(hfac)_2$ with nitroxides allowed us to divide the nitroxides under consideration into two groups. Nitroxides $\mathbf{L^1}$—$\mathbf{L^3}$ form complexes as a result of monodentate coordination through the nitrogen atom of the tetrazole ring, whereas $\mathbf{L^4}$ is involved in bidentate coordination through the imine nitrogen atoms of the 2-imidazoline and tetrazole rings. Coordination of the nitrogen atom of the imino nitroxide fragment in complex **4** results in strong intramolecular ferromagnetic exchange interactions between the unpaired electrons of the paramagnetic centers.

Experimental

The IR spectra were recorded on a Bruker VECTOR 22 spectrometer (KBr pellets). Elemental analysis was carried out on a Carlo-Erba C,H,N-analyzer at the Vorozhtsov Novosibirsk Institute of Organic Chemistry of the Siberian Branch of the Russian Academy of Sciences. The magnetic measurements were performed on a SQUID MPMS-5S (Quantum Desing) magnetometer in the temperature range of 2—300 K in magnetic field of 5 kOe.

4,4,5,5-Tetramethyl-2-(1-methyl-1*H*-tetrazol-5-yl)-4,5-dihydro-1*H*-imidazole-1-oxyl 3-oxide ($\mathbf{L^1}$) and 4,4,5,5-tetramethyl-2-(2-methyl-1*H*-tetrazol-5-yl)-4,5-dihydro-1*H*-imidazole-1-oxyl 3-oxide ($\mathbf{L^2}$). A mixture of 2-cyano-4,4,5,5-tetramethyl-4,5-dihydro-1*H*-imidazole 1-oxide[2] **A** (0.72 g, 4.0 mmol), NaN_3 (0.28 g, 4.3 mmol), NH_4Cl (2 mg, 0.04 mmol), and DMF (8 mL) was stirred at 60—65 °C for 3 h until the starting nitroxide **A** was consumed. Then the temperature of the reaction mixture was lowered to 50 °C, and Me_2SO_4 (380 μL, 0.5 g, 4 mmol) was added in one portion. The reaction mixture was stirred for 20 min, DMF was distilled off, and the solid residue was treated portionwise with $CHCl_3$ (~3×20 mL). The chloroform extracts were combined and concentrated to dryness. The resulting blue powder was dissolved in an ethyl acetate—hexane mixture at ~50 °C. The mixture was filtered and slowly cooled. The crystals of $\mathbf{L^1}$ that formed were filtered off. The filtrate was concentrated and the residue was again recrystallized, due to which an additional amount of nitroxide $\mathbf{L^1}$ was obtained. The filtrate obtained after crystallization was concentrated to dryness, and the residue was chromatographed on a silica gel column (1.5×30 cm) using successively a mixture of ethyl acetate with benzene (1 : 10, v/v) and then ethyl acetate. A violet fraction containing $\mathbf{L^1}$ and then a fraction containing $\mathbf{L^2}$ were collected. The total yields of $\mathbf{L^1}$ and $\mathbf{L^2}$ were 0.63 g (66%) and 0.19 g (20%), respectively. The melting points and the IR spectra of samples of $\mathbf{L^1}$ and $\mathbf{L^2}$ were identical to those described earlier.[3]

4,4,5,5-Tetramethyl-2-(1-methyl-1*H*-tetrazol-5-yl)-4,5-dihydro-1*H*-imidazole 1-oxide ($\mathbf{L^3}$) was prepared by the reaction of $NaNO_2$ and AcOH with $\mathbf{L^1}$ in a two-phase $CHCl_3$—water system.[6] Crystals suitable for X-ray diffraction study were grown from a CH_2Cl_2—heptane mixture. The yield was 0.22 g (77%), orange crystals, m.p. 120—121 °C, μ_{eff} = 1.73 μ_B (295 K). Found (%): C, 48.1; H, 6.8; N, 37.7. $C_9H_{15}N_6O$. Calculated (%): C, 48.4; H, 6.8; N, 37.6. IR, ν/cm^{-1}: 639, 698, 834, 876, 964, 1132, 1148, 1167, 1206, 1225, 1263, 1305, 1371, 1432, 1458, 1611, 2873, 2979.

4,4,5,5-Tetramethyl-2-(2-methyl-1*H*-tetrazol-5-yl)-4,5-dihydro-1*H*-imidazole 1-oxide ($\mathbf{L^4}$) was prepared analogously to $\mathbf{L^3}$ from nitronyl nitroxide $\mathbf{L^2}$. The yield was 83 mg (89%), orange crystals, m.p. 82—83 °C, μ_{eff} = 1.72 μ_B (295 K). Found (%): C, 48.6; H, 6.8; N, 37.9. $C_9H_{15}N_6O$. Calculated (%): C, 48.4; H, 6.8; N, 37.6. IR, ν/cm^{-1}: 645, 705, 835, 871, 958, 1026, 1071, 1147, 1188, 1232, 1270, 1369, 1395, 1433, 1458, 1600, 2966, 2987.

Complex $Cu(hfac)_2\mathbf{L^1}_2$ (1). A mixture of $Cu(hfac)_2$ (0.0500 g, 0.10 mmol) and $\mathbf{L^1}$ (0.0500 g, 0.21 mmol) was dissolved in CH_2Cl_2 (10 mL), and hexane (5 mL) was added to the resulting dark-brown solution. After 4 h, dichroic crystals (maroon and dark-green faces in reflected light) were obtained. The compound was filtered off, washed with hexane, and dried in air. The yield was 75%. Found (%): C, 35.9; H, 3.5; N, 17.4; F, 24.3. $C_{28}H_{32}O_8F_{12}N_{12}Cu$. Calculated (%): C, 35.2; H, 3.4; N, 17.6; F, 23.8.

Complex $Cu(hfac)_2\mathbf{L^2}_2$ (2). A mixture of $Cu(hfac)_2$ (0.0500 g, 0.10 mmol) and $\mathbf{L^2}$ (0.0500 g, 0.21 mmol) was dissolved in CH_2Cl_2 (2 mL). Hexane (5 mL) was added to the resulting dark-brown solution. Then the solution was slowly concentrated to 5 mL in an air flow. The crystalline brown compound that formed was filtered off, washed with hexane, and dried in air. The yield was 30%. Solutions of complex **2** are unstable. Found (%): C, 35.1; H, 3.1; N, 16.9; F, 24.2. $C_{28}H_{32}O_8F_{12}N_{12}Cu$. Calculated (%): C, 35.2; H, 3.4; N, 17.6; F, 23.8.

Complex $Cu(hfac)_2\mathbf{L^3}_2$ (3). A mixture of $Cu(hfac)_2$ (0.0642 g, 0.13 mmol) and $\mathbf{L^3}$ (0.0300 g, 0.13 mmol) was dissolved in diethyl ether (2 mL). Hexane (5 mL) was added to the resulting dark-brown solution. After 1 day, large pale-brown crystals precipitated. The compound was filtered off, washed with hexane, and dried in air. The yield was 80%. Found (%): C, 36.6; H, 3.2; N, 18.0; F, 25.8. $C_{28}H_{32}O_6F_{12}N_{12}Cu$. Calculated (%): C, 36.4; H, 3.5; N, 18.2; F, 24.7.

Complex $Cu(hfac)_2\mathbf{L^4}$ (4). A mixture of $Cu(hfac)_2$ (0.0539 g, 0.11 mmol) and $\mathbf{L^4}$ (0.0250 g, 0.11 mmol) was dissolved in hexane (6 mL) with heating to 60 °C for 10—15 min. The resulting yellow-green solution was kept at room temperature for 30 min. The crystals that formed were filtered off, washed with hexane, and dried in air. The yield was 22%. Found (%): C, 33.1; H, 2.6; N, 12.5; F, 32.9. $C_{19}H_{17}O_5F_{12}N_6Cu$. Calculated (%): C, 32.6; H, 2.4; N, 12.0; F, 32.5. The resulting solid phase

Table 4. Crystallographic data and details of X-ray diffraction studies

Parameter*	L^3	L^4	**1**	**3**	**4a**	**4b**	**4c**
Molecular weight	223.27	223.27	956.20	924.20	700.93	700.93	700.93
Crystal system	Triclinic	Triclinic	Triclinic	Triclinic	Monoclinic	Triclinic	Triclinic
Space group	$P\bar{1}$	$P\bar{1}$	$P\bar{1}$	$P\bar{1}$	$P2_1/c$	$P\bar{1}$	$P\bar{1}$
a/Å	10.022(2)	9.937(2)	9.8498(13)	9.8737(18)	10.2236(9)	8.9860(12)	9.3150(13)
b/Å	10.497(2)	9.939(3)	10.9308(15)	10.9168(19)	22.139(2)	10.2046(14)	10.3262(14)
c/Å	12.252(3)	12.716(3)	11.1024(15)	10.989(2)	24.890(2)	15.559(2)	15.599(2)
α/deg	90.161(4)	101.776(5)	66.281(2)	66.956(3)	—	106.568(2)	73.286(2)
β/deg	104.344(4)	90.125(6)	76.088(2)	63.692(3)	94.236(2)	94.236(2)	85.617(2)
γ/deg	108.038(4)	107.151(5)	64.460(2)	76.224(3)	—	90.081(2)	83.698(2)
V/Å^3	1182.8(4)	1172.2(5)	984.2(2)	974.1(3)	5618.1(9)	1366.5(3)	1426.8(3)
Z	4	4	1	1	8	2	2
d_{calc}/g cm^{-3}	1.254	1.265	1.613	1.576	1.657	1.703	1.627
μ/mm^{-1}	0.089	0.090	0.674	0.675	0.898	0.923	0.882
Scan range, θ/deg	1.72—3.38	1.64—23.27	2.51—23.31	2.03—23.27	1.84—23.27	2.08—23.28	2.07—23.30
Number of reflections							
measured	5204	5082	4312	4239	23770	5619	11110
independent	3400	3342	2811	2783	8061	3890	4128
R_{int}	0.0637	0.0743	0.0482	0.0812	0.0422	0.0402	0.0683
Number of parameters in refinement	401	410	369	387	912	511	497
GOOF	0.575	0.676	0.844	0.779	1.013	0.755	0.811
R factors based on reflections with $I > 2\sigma(I)$:							
R_1	0.0496	0.0614	0.0409	0.0388	0.0620	0.0396	0.0500
wR_2	0.1380	0.1261	0.0871	0.1008	0.1475	0.1051	0.1275
R factors (all reflections):							
R_1	0.0794	0.1597	0.0570	0.0502	0.0836	0.0461	0.0738
wR_2	0.1729	0.1712	0.0949	0.1086	0.1607	0.1125	0.1441

* The molecular formulas: $C_9H_{15}N_6O$ (L^3 and L^4), $C_{28}H_{32}CuF_{12}N_{12}O_8$ (**1**), $C_{28}H_{32}CuF_{12}N_{12}O_6$ (**3**), and $C_{19}H_{17}CuF_{12}N_6O_5$ (**4a—c**).

contained two types of crystals, *viz.*, green elongated prisms (**4a**) and dichroic (green and brown faces in reflected light) prisms (**4b**). The mother liquor was heated at 50—60 °C for 30—40 min. The reaction mixture turned yellow-brown. After its storage at room temperature for ≥3 h, pale-brown platelet crystals of complex **4c** were obtained. Found (%): C, 33.0; H, 2.3; N, 12.1; F, 31.8. $C_{19}H_{17}O_5F_{12}N_6Cu$. Calculated (%): C, 32.6; H, 2.4; N, 12.0; F, 32.5.

X-ray diffraction study. X-ray diffraction data sets were collected from single crystals on an automated SMART APEX CCD (Bruker AXS) diffractometer (Mo-Kα, λ = 0.71073 Å, room temperature). Absorption correction were applied using the Bruker SADABS software (version 2.03). The structures were solved by direct methods and refined by the full-matrix least-squares method with anisotropic displacement parameters for all nonhydrogen atoms. The positions of the H atoms, except for the H atoms of the Me groups, were calculated theoretically. The H atoms of the Me groups were refined isotropically in the rigid-body approximation. All calculations associated with the structure solution and refinement were carried out with the use of the SHELX-97 and Bruker SHELXTL Version 6.12 program packages. The crystallographic data are given in Table 4.

Magnetic measurements. The paramagnetic component of the magnetic susceptibility χ was calculated taking into account the additive diamagnetic contribution in accordance with the Pascal constants. The temperature dependence of the effective magnetic moment was calculated by the equation

$$\mu_{eff}(T) = \left(\frac{3k}{N\mu_\beta{}^2}\cdot\chi T\right)^{1/2} \approx (8\chi T)^{1/2},$$

where N is Avogadro's number, k is the Boltzmann constant, and β is the Bohr magneton.

This study was financially supported by the Russian Foundation for Basic Research (Project Nos 03-03-32158, 04-03-08002, and 05-03-32305), the US Civilian Research and Development Foundation (CRDF, Grant Y1-C-08-03), the Russian Science Support Foundation, the Russian Academy of Sciences, the Siberian Branch of the Russian Academy of Sciences, and the Bruker.

References

1. *Proc. IX Intern. Conf. on Molecule-based Magnets (Tsukuba, 4—8 October, 2004)*, Japan, 2004.
2. E. V. Tretyakov, O. V. Koreneva, G. V. Romanenko, Yu. G. Shvedenkov, and V. I. Ovcharenko, *Polyhedron*, 2004, **23**, 763.
3. E. V. Tretyakov, S. V. Fokin, G. V. Romanenko, and V. I. Ovcharenko, *Polyhedron*, 2003, **22**, 1965.
4. (a) E. V. Tretyakov, G. V. Romanenko, and V. I. Ovcharenko, *Tetrahedron*, 2004, **60**, 99; (b) E. V. Tretyakov, G. V. Romanenko, Yu. G. Shvedenkov, V. I. Ovcharenko, and R. Z. Sagdeev, *Izv. Akad. Nauk, Ser. Khim.*, 2004, 1248 [*Russ. Chem. Bull., Int. Ed*., 2004, **53**, 1301].
5. I. V. Ovcharenko, Yu. G. Shvedenkov, R. N. Musin, and V. N. Ikorskii, *Zh. Strukt. Khim.,* 1999, **40**, 36 [*Russ. J. Struct. Chem*., 1999, **40** (Engl. Transl.)].
6. E. F. Ullman, L. Call, and J. H. Osiecki, *J. Org. Chem*., 1970, **35**, 3623.

Received December 9, 2005